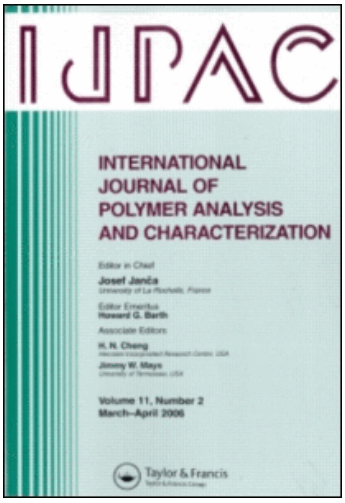

International Journal of Polymer Analysis and Characterization
Publication details, including instructions for authors and subscription information:
http://www.informaworld.com/smpp/title~content=t713646643

Polymer Nanoparticle Characterization in Aqueous Suspensions

Cécile Duclairoir[a]; Evelyne Nakache[a]
[a] Equipe Polyme'res-Interfaces, ISMRa, Caen Cedex, France

Online publication date: 27 October 2010

To cite this Article Duclairoir, Cécile and Nakache, Evelyne(2002) 'Polymer Nanoparticle Characterization in Aqueous Suspensions', International Journal of Polymer Analysis and Characterization, 7: 4, 284 — 313
To link to this Article: DOI: 10.1080/10236660213159
URL: http://dx.doi.org/10.1080/10236660213159

International Journal of Polymer Anal. Charact., 7: 284–313, 2002

1023-666X/02 $12.00 + .00
DOI: 10.1080/10236660290026511

Polymer Nanoparticle Characterization in Aqueous Suspensions

Cécile Duclairoir and Evelyne Nakache
Equipe Polymères-Interfaces, ISMRa, Caen Cedex, France

This article evaluates several techniques for measuring nanoparticle size in suspension. The direct techniques measure the nanoparticle size by electron microscopy. However, with this technique, the particles must be observed dry, except in the case of environmental microscopy, and their distribution is calculated by performing image analysis. Other indirect methods, based on measurements of intensity fluctuations allow size measurement but these methods are dependent on sample preparation (concentration, polydispersity, etc.). Two types of materials are characterized and discussed herein: model polystyrene latex particles used for size standardization in several devices and polydisperse wheat protein nanoparticles prepared in our laboratory. Our results show that no size characterization method is totally universal and absolute. Coupling at least two different methods allows for more rigorous size characterization.

Keywords: Size characterization techniques; Nanoparticles; Suspension; Polydispersity; Multimodal

Received 12 July 2000; accepted 15 February 2001.

Financial support of Matériaux-Polymeres-Plasturgie Network of Normandie, France, is acknowledged. The authors are gratefully indebted for fruitful discussions and technical help to Dr. D. Renard, INRA of Nantes LPCM, LS and Laser Granulometry; Dr. P. Depraetere and M. Massard ERA Zétamétrie of Caen University; M. Vizcaïno, Sté Séphy (DLS device); and Dr. F. Osterstock, LERMAT ISMRa (SEM).

Address correspondence to Dr. Cécile Duclairoir, Laboratoire de Microbiologie du Froid, IUT d' Evreux, 55 rue Saint Germain, Evreux, 27000, France. E-mail: cecile.duclairoir@univ-rouen.fr

Nowadays, polymer colloids are of great interest in many fields: drug vectorization, agrochemistry, varnishes, paints, inks, and so on. Their industrial use is related to their efficiency, which is a function of several parameters: their particle size, surface properties, loading capacity, and release capacity. In pharmaceutical applications, for instance, submicronic vectors such as drug loaded polymer nanoparticles have to reach the extremity of the smallest blood capillaries, whose diameter is about 4 μm. Their small sizes are therefore obviously of great importance.

Numerous techniques have been used to characterize colloids, but their applications may be limited by theoretical considerations or by experimental limitations. The purpose of this article is, first, to review some size characterization techniques used to characterize nano- or microparticles. Some techniques (light scattering, laser granulometry, electron microscopy) will be described extensively. This presentation will also discuss, in a less systematic way, the applications of the Coulter counter, ultrasonic or confocal microscopy, and sedimentation techniques. Second, we will illustrate some of these techniques by analyzing data on very dilute suspension of standard latexes and plant protein nanoparticles[1], studied in our laboratory. Both theoretical background and practical applications will be discussed here. Usually nanoparticles are formed from synthetic polymers, but they may also be formed from animal proteins. The nanoparticles studied herein are biocompatible, biodegradable, and, contrarily to animal proteins, they are free from prions.

The sample polydispersity is also a very important parameter, but it can be hard to estimate. We will discuss here how to overcome this difficulty.

REVIEW OF NANOPARTICLES SIZE CHARACTERIZATION TECHNIQUES IN AQUEOUS SUSPENSIONS

Methods for measuring nanoparticle size may be divided into two categories: nondestructive methods and destructive methods. These methods may also be categorized according to practical advantages and disadvantages, such as limitations on size range, etc.

Nondestructive Methods

The nondestructive techniques allow the study of particles in an aqueous medium, which may or may not be diluted. For easy size characterization, the sample must be either monomodal (a unique size distribution) or multimodal (several size classes) with a limited polydispersity (narrow size distribution).

Light Scattering

Light scattering (LS) requires the use of highly diluted samples in order to avoid multiple scattering. The particles in suspension are subjected to Brownian motion and scatter[2] the monochromatic incident light (wavelength λ) in the diffusion volume shown in Figure 1[3]. In order to avoid particle interactions, the sample has to be highly diluted with the continuous phase of the suspension. In such an ideal case without any particle interactions, the intensity fluctuations are collected by a photodetector. The data may be treated in two ways:

- Data averaged over a period of time: so-called dynamic light scattering (SLS)
- Time dependent acquisition: so-called dynamic light scattering (DLS) and then fitted by theoretical models

When a size determination is carried out by LS, it can be difficult to choose the best algorithm to use for the interpretation of the data. These algorithms will be discussed in the sample studies section. Nowadays, any LS apparatus gives a size evaluation, but care must taken to assure proper data interpretation. Rayleigh[4], considering time-averaged scattering of isolated spherical scatterers, treated the simplest case. Rayleigh scattering only applies to particles smaller than $\lambda/20$[5]. When particles are larger than about $\lambda/20$, the method commonly called SLS gives the radius of gyration, the molecular weight and the second virial coefficient

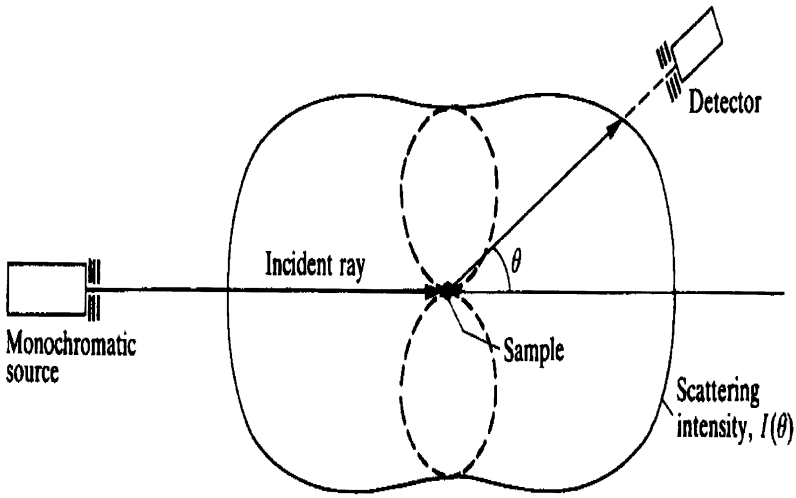

FIGURE 1 Light scattering device (courtesy of Oxford University Press[3]).

of the polymer. By a more complex approach, Rayleigh–Gans–Debye theory[6, 7], investigates particles in interaction in a diluted medium. Sizes up to $\lambda/2$ can be measured. The usual incident light is a red or green laser (λ is less than 640 nm), so the biggest observed size is about 300 nm[5].

DLS is a broadly applied size characterization technique, also known as photon correlation spectroscopy (PCS) or quasi-elastic light scattering (QELS). By this technique, the intensity fluctuations are fitted, with the help of a correlator, by an autocorrelation function G_1 as a function of time (Eq. 1).

$$G_1(t) = \exp\left(-Dq^2t\right) \tag{1}$$

with D the translational diffusion coefficient, n solvent refractive index, and λ the wavelength of the incident beam. The wave vector q is given by

$$q = \frac{4\pi n}{\lambda} \sin\left(\frac{\theta}{2}\right) \tag{2}$$

with θ the observation scattering angle and n the refractive index of the medium. Different algorithms or theoretical models can be used for data treatment and by Stokes law and Einstein's equation of Brownian motion, they can yield the diffusion coefficient D and, consequently, the hydrodynamic radius R_h (radius of sphere having the same diffusion coefficient as the polymer) as given in Equation 3.

$$R_h = \frac{kT}{6\pi\eta D} \tag{3}$$

with k the Boltzman constant, T the absolute temperature, and η the sample viscosity. No calibration is needed, and the measured value is absolute. For spherical particles smaller than $\lambda/2$, a single measurement at 90° is sufficient, although for polydisperse materials angular dependence on the measured D values may be observed.

In the two LS methods, plots of the particle diameter versus the size distribution are generated as shown later in the sample studies. These two approaches do not take into account the angular dependency of the intensity fluctuations, even if they are accumulated at different angles between 30° and 150°. For larger particles, which are bigger than λ, the intensity fluctuations depend dramatically on the observation angle. The Mie theory[8], based on refractive index fluctuations, covers up this angular dependence and gives the closest size classes to the real size distribution. The two LS approaches diverge from each other for particle size greater than 350 nm (i.e., $\lambda/2$) and the differences increase dramatically. For instance, for a same relative scattering intensity at 90°, the displacement could reach more than 100 nm for submicronic particles.

The Mie theory allows the observation of particles of, at least, a few micrometers.

The DLS drawbacks are as follows:

- Several angle acquisitions are necessary, except for spherical particles. In that case, acquisition at a single angle of 90° is enough.
- The preparative conditions must avoid any pollutant such as oil on the glassware or ambient dust during experiments and even before. The glassware has to be cleaned carefully with sulfochromide or surfactant mixtures and solvents have to be filtered.
- The sample has to be very diluted, which may provoke a dilution shock. A slightly blue coloration appears for very diluted suspensions of particles smaller than the light wavelength.
- Numerous algorithms are necessary to interpret light fluctuations and to discriminate their various meanings.
- The proportions of the different size classes are related to peak areas, and, due to theoretical assumptions, they could diverge from reality.

Laser Granulometry

Laser granulometry is based on light diffraction by a beam whose λ is smaller than the particle size. The particle refractive index must be different from that of the aqueous medium. A concentric annular detector at small angles collects the diffracted light. The difference between the refractive indexes of the particles and the medium leads to the particle size. The study of the intensity fluctuations allows measurements of the size distribution, $X(d)$, as given by Eq. (4) with the help of Mie theory[8].

$$X(d) = N\sum_{n=1}^{\infty}[(2n+1)/(n(n+1))]\{a_n\pi_n(\cos\theta) + b_n\tau_n(\cos\theta)\} \times (-1)^{n+1} \tag{4}$$

where π_n and τ_n are related to Legendre polynomials as given in Eqs. (5*a*) and (5*b*)

$$\pi_n(\cos\theta) = P_n^{(1)}(\cos\theta)/\sin\theta \tag{5a}$$

and

$$\tau_n(\cos\theta) = \frac{d}{d\theta}(P_n^{(1)}(\cos\theta)) \tag{5b}$$

and a_n and b_n are dependent on the particle size, d, and on the relative refractive index of the particles to their medium, m, as shown in Eqs. (6*a*) and (6*b*).

$$a_n = \{\Psi_n(\alpha)\Psi_n(\beta) - m\Psi_n(\beta)\Psi_n(\alpha)\}/\{\zeta_n(\alpha)\zeta_n(\beta) - m\zeta_n(\beta)\zeta_n(\alpha)\} \tag{6a}$$

$$b_n = \{m\Psi_n(\alpha)\Psi_n(\beta) - \Psi_n(\beta)\Psi_n(\alpha)\}/\{m\zeta_n(\alpha)\zeta_n(\beta) - \zeta_n(\beta)\zeta_n(\alpha)\} \quad (6b)$$

with $\alpha = 2\pi d/\lambda$ and $\beta = m\alpha$ and Ψ Ricatti–Bessel functions and ζ Hankel functions.

A lens with a focal length of 45 μm situated between the incident beam and the sample cell, as shown on Figure 2, allows the observation of particles between 0.1 and 80 μm and a lens with a focal length of 100 μm positioned after the sample cell and before the detector, as represented in Figure 3, characterizes sizes from 0.5 to 170 μm. Thus different optical systems allow the measurement of different size ranges.

Laser granulometry requires some caution during sample preparation:

- Elimination of dust (glassware cleaning, filtered solvents, etc.)
- Use of the ideal sample concentration, which is often a balance between a limited sample quantity and systematic dilution. This dilution may disturb particle stability. Usually, prior to the measure, a concentration test is done by the estimation of an obscuration factor of the suspension.
- Prevention of possible gas bubbles during the stirring or ultrasonication of the sample

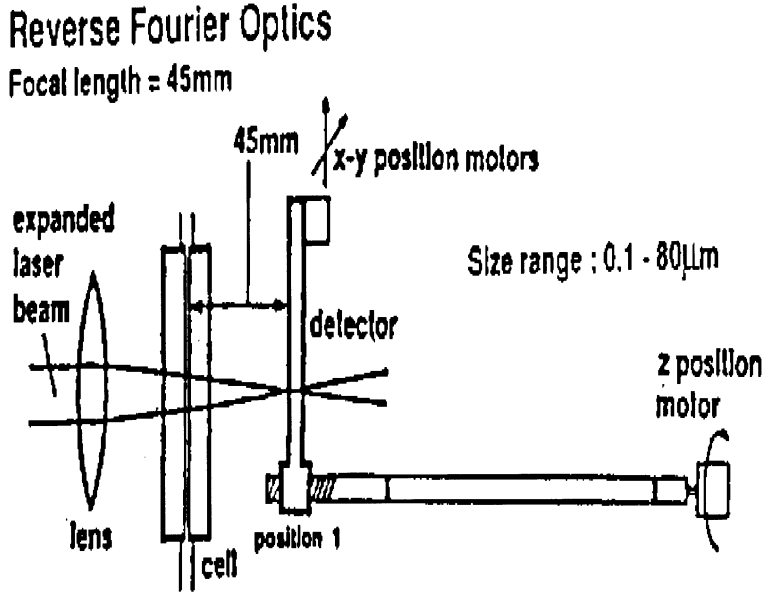

FIGURE 2 Laser granulometry device: 45 mm lens focal (courtesy of Malvern Instrument Limited).

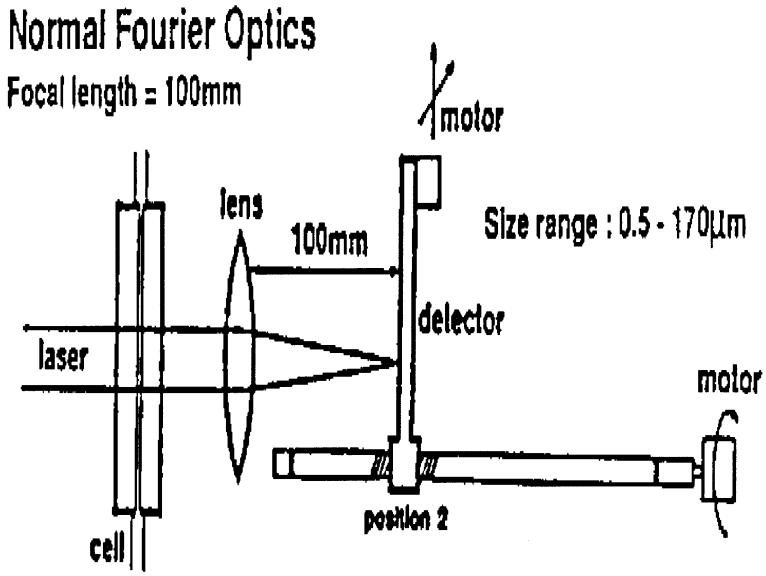

FIGURE 3 Laser granulometry device: 100 mm focal lens (courtesy of Malvern Instrument Limited).

The resulting plot is similar to the plot generated in DLS: size distribution vs. volume-average diameters.

Coulter Counter

Largely used by the paint and pharmaceutical industries, this method is an electronic size measuring technique. It is based on the Coulter principle[9] of allowing the dispersion to flow through a narrow aperture, where particles cause a change in the conductivity of the medium (see Figure 4). This conductivity variation, R, is a function of particle diameter, d, and its volume, V, as shown in Eq. (7).

$$R = \frac{\frac{r_e V}{A^2}\left(1 - \frac{r_e}{r_p}\right)}{1 - \left(1 - \frac{r_e}{r_p}\right)\frac{d}{A}} \tag{7}$$

with A the aperture section, r_e the electrolyte resistivity, r_p particle resistivity. This method is not very sensitive to submicron sized particles. This instrument was one of the first particle size instruments on the market and it is simple and quick to use.

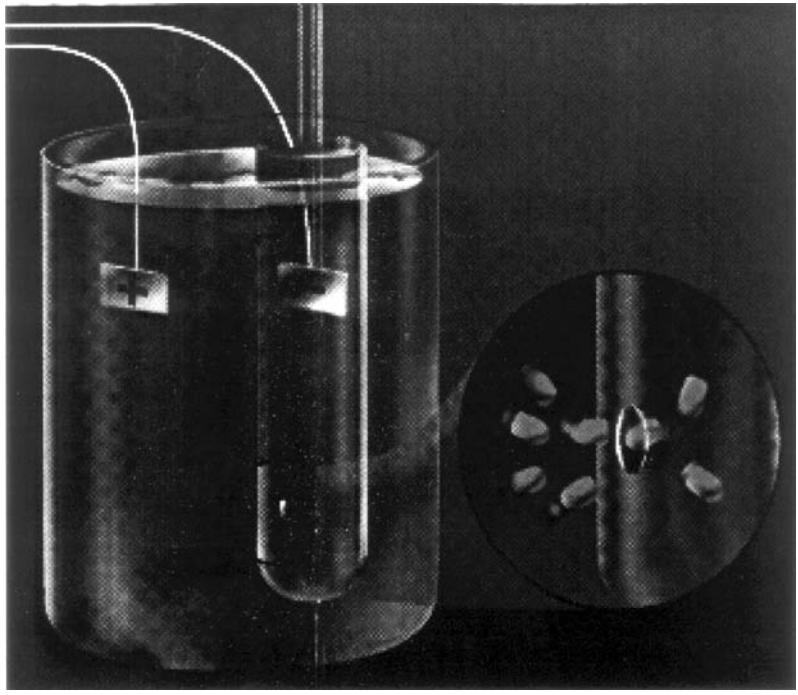

FIGURE 4 Scheme of Coulter counter apparatus (courtesy of Micromeritics).

The drawbacks are encountered in the following:

- The sample preparation must be without pollutant (i.e., oil on the glassware or ambient dust).
- The difference in the conductivity between particles and the medium has to be significant. The ideal case consists of a conducting medium with a nonconducting particle.

Ultrasonic Spectroscopy

Since the beginning of the 1990s, vesicle and polymer particle diameters have been measured by ultrasonic velocity[10]. In the emulsion domain, this technique is very common and facilitates size investigation from 10 nm to 1,000 μm. For high frequencies (i.e., study of large particles), the ultrasound can be destructive, so this method should be used with caution. This is especially the case for fragile objects such as vesicles or emulsions.

The main advantage of this technique is its application to concentrated particle suspensions. Caution has to be observed in preparing samples without gas bubbles, which may disturb ultrasonic wave displacement.

Confocal Microscopy

Confocal fluorescent microscopy[11] involves the study of labeled core particles. It can be easily achieved with the help of fluorescent markers for polymerized particles. In confocal microscopy, all objects out of focus are suppressed from image formation. The minimum measured size is 200 nm. Three-dimensional representations can be built up from two-dimensional image analyses.

By such microscopy, very small quantities, even of polydisperse samples, can be observed. This technique also generates very high quality reflected images in brightfield. The disadvantages are necessary fluorescent core and matching solvent in order to reduce light scattering.

Environmental Microscopy

This most recent technique is based on scanning electronic microscopy, but the aqueous environment of the particles is preserved (no need to dry sample). Performing measurements involves exposing a drop of the solution sample to an electron beam with a pressure gradient in the specimen chamber, as shown in Figure 5[12]. This allows a sufficient sample hydration instead of the high vacuum required in traditional electronical microscopies. Following irradiation, the sample emits secondary electrons collected by a detector, as shown in Figure 6. Their topography is observed in the sample micrograph. Recent work has shown that by minimizing the electron beam path through the vapor and by working at the lowest acceptable pressure, remote electron scattering and artifact X-ray production can be reduced to an acceptable level[13]. This technique is suitable for characterizing polydisperse sample.

Sedimentation

The theory and practice of free sedimentation are ruled by the well-known Stokes law. Free sedimentation means that a particle sediments in a manner independent of the neighboring particles[5]. The heavier the particle is, the shorter the sedimentation time is.

Traditional sedimentation. Gravity-induced sedimentation is too slow with submicronic objects. In fact, Brownian motion for such particles is very important and disturbs the sedimentation kinetics. As a consequence, centrifugation and ultracentrifugation are employed.

Centrifugation and ultracentrifugation. These methods separate particles into size classes by sedimentation resulting from the earth's gravity

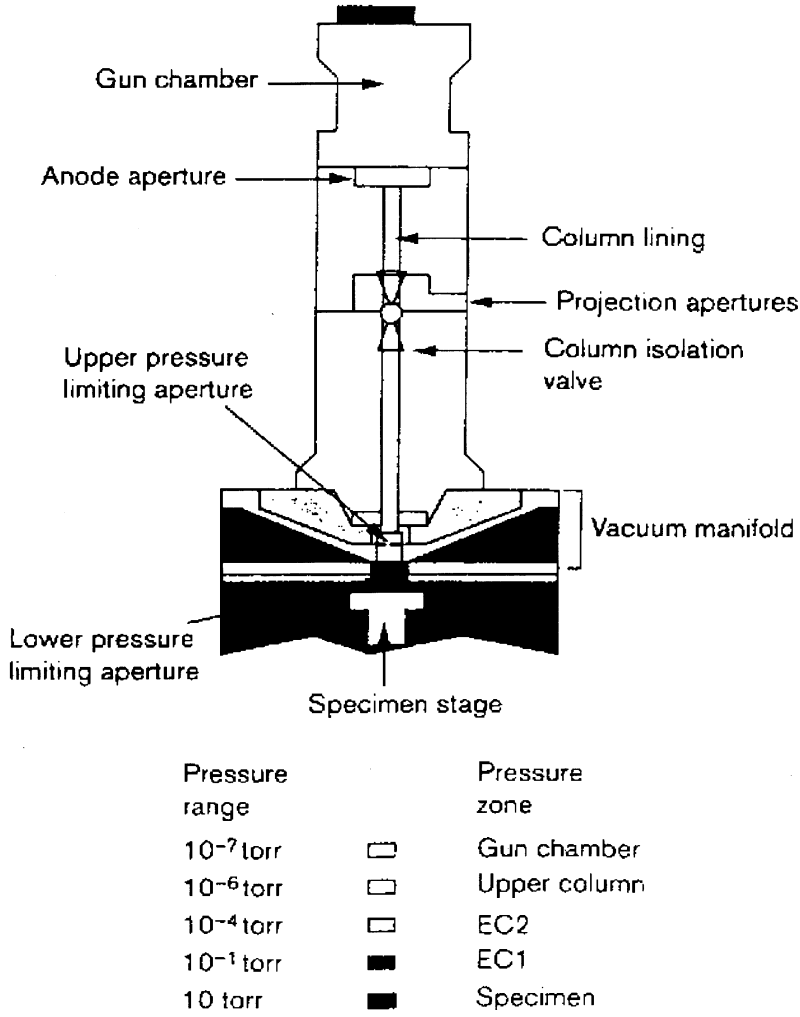

FIGURE 5 Environmental scanning, electronical microscopy apparatus (courtesy of Elsevier Science Editors[12]).

and centrifugal acceleration. An optical system is generally used to detect the displacement of the sedimentation front. The centrifugal speed is less than 10,000 rpm for centrifugation. The minimum particle size is 250 nm[9]. With ultracentrifugation, for inorganic particles, the accessible size can be as small as a few nanometers[14].

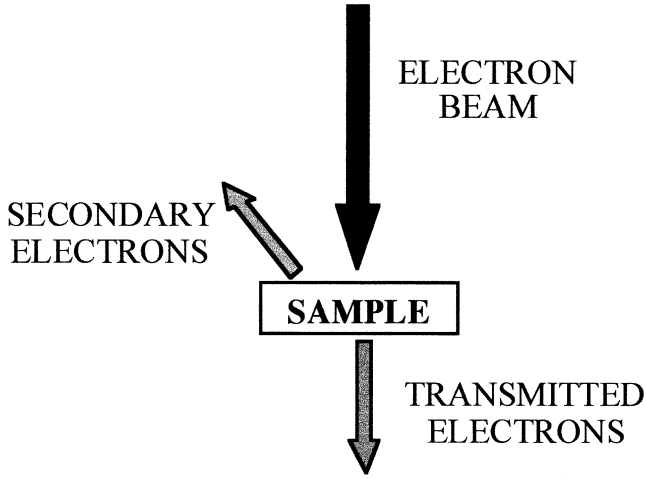

FIGURE 6 Sample submitting to an electronic beam.

The drawbacks are as follows:

- Nonspherical particles require a more complex treatment.
- Hard particles are required because of strength of the centrifugal field, which may deform soft particles.
- Finding an adequate optical system, particularly in the case of turbid suspensions.
- Several dilutions may be necessary in order to avoid particle interactions. Optimal concentration up to 1% (v/v) is usually obtained[9].

1. Destructive Methods

With destructive methods the particles are removed from the aqueous environment.

Electron Microscopy

Electron microscopy[15] is a common name for several techniques where the sample is submitted to an electron beam of modulated power. In the observation chamber the pressure conditions are strictly controlled, and most measurements are performed under vacuum. A scanning electron microscopy (SEM) micrograph is a topography of the intensity of the secondary electrons. For transmission electron microscopy (TEM), the intensity of the transmitted electrons is collected (see Figure 6). The size range and resolution of these techniques are

dependent on the beam power. For example, 20 kV is enough to observe submicronic particles with a resolution of 50 nm.The sample preparation is specific to each technique. By these methods, an image of the particles themselves is obtained. A mean size characterization requires an image analysis, which must be more elaborate if the sample is polydisperse. In the latter case, the mean diameter is normally calculated as a number-averaged diameter. One has to be aware that the electron beam can fuse particles, such as polymer gels.

Scanning Electron Microscopy (SEM)

The "dried" sample is submitted to an electron beam and the topography of secondary electron intensity leads to particle size evaluation. The smallest observed particles are about 200 nm. The preparation method of the "dried" sample leads to the distinction between classical and cryofracture methods.

In the classical case, the aqueous sample is placed on a sample-support and evaporated under vacuum before covering it with colloidal metal. In cryofracture SEC, the aqueous sample is frozen by immersion in liquid nitrogen prior to fracturing. It is then submitting to a gentle cleaning of the fracture plane surface. The ice quality is of great importance; it has to be amorphous to form the best replica of the surface.

Platinum, then carbon are deposited in order to obtain a rigid and SEM observable replica.

Cryofracture TEM

Several preparation methods may be employed depending on the nature of the sample.

- Small drops of the sample are projected onto a cryogenically cooled metal surface and mechanically fractured afterward. A replica is formed by metal vapor deposition and then submitted to the electron beam.
- A thin layer of the sample is frozen and then submitted to the electron beam. The transmitted electrons are collected to evaluate their intensity topography. The sample is frozen so rapidly that amorphous and transparent ice is formed.

Scanning Tunneling Microscopy (STM) and Atomic Force Microscopy (AFM)

The "hydrated" and slightly conductive sample, where the solvent is not completely evaporated, can be studied with the help of a sharp metal tip bound to a piezoelectric crystal.

For STM[15], the sample surface has to be conducting or metallized. A voltage increase of the piezocrystal moves the tip to a distance where a tunneling current is detected. For AFM[15], the tip scans over the surface

and its deflections are detected by a laser system on its backside. The size resolution is less than one nanometer. The main disadvantage is that the tip cannot scan convex topology. In this case, tapping (push and pull STM) may be used, which allows measurements of diameters.

Let us now give some examples of experimental measurements in order to illustrate some of these techniques and how to choose the appropriate one.

STUDY OF AN IDEAL SAMPLE: LATEXES

The first example is a standard sample of calibrated polystyrene nanoparticles, provided by Interfacial Dynamics Corp. (Portland, Oregon, USA). The number-average diameter was given as 310 (± 10) nm (based upon TEM). This ideal suspension was characterized by three techniques: DLS, laser granulometry, and SEM.

DLS Study

The complete DLS study was performed on a SEMATech photogoniometer (Nice, France) with the help of a Malvern 7032CN correlator (Malvern, Worcestershire, UK). The Malvern software PCS 1.32 was used to analyze the data. As stated earlier, the sample preparation has to be done with caution (no dust, contaminants, or multiple scattering).

For each sample, at least five acquisitions of ten sub-runs were made. The software for each subacquisition checks off the measurement quality for each mathematical treatment (monomodal-cumulants, Contin described later). The intensity ratio suspension/solvent has to be more than ten. In our case, it is fifty times larger.

The correlator gives results that are highly dependent on the chosen algorithm (i.e., a mathematical model) and the different theoretical approaches: monomodal-cumulants, Contin, non-negatively constrained least squared (NNLS), inverse Laplace transformation (ILT), and so on. Several such methods are described in the literature, especially in an exhaustive review by Stepanek[16]. Here, monomodal-cumulants and Contin treatments are presented, since they are the most used routine algorithms.

Each algorithm induces some assumptions about the sample composition and its polydispersity. The monomodal algorithm assumes nothing about the distribution. It consists in fitting a polynomial to the log of the normalized correlation function. Contin mode, developed by the Provencher team[17], analyses the correlation through an inverse transformation. Its consists in adding a constraint—the regulariser—to an ordinary least-squares criteria for achieving the best fit. This mode is convenient for several populations. An automatic mode exists, which is a

combination of monomodal and Contin mode with a priority to the monomodal.

In Table I various averaged diameters obtained by different analysis are compiled.

Three average diameters can be obtained:

- Intensity-average, d_I, (also called z-average diameter) calculated by

$$d_I = \frac{\sum_i n_i d_i^7}{\sum_i n_i d_i^6} \tag{8}$$

  with n_i the relative particle proportion in the corresponding class size d_i
- Volume-average, d_v, (also called weight-average) is obtained by assuming that the particles are spherical and multiplying the relative contribution of each size class d_i by the volume corresponding to a sphere in that size class

$$d_v = \frac{\sum_i n_i d_i^4}{\sum_i n_i d_i^3} \tag{9}$$

- Number-average, d_n obtained with the help of

$$d_n = \frac{\sum_i n_i d_i}{\sum_i n_i} \tag{10}$$

In the case of particle diameters larger than λ, a part of the light is adsorbed and the intensity average diameter estimation is a function of the particle refractive index which has to be known precisely. Then, the other average representations are calculated by the chosen method (Eqs. 8–10). Thus, if the refractive index is not properly defined, these average-diameters can be erroneous.

The intensity value is more appropriate for reporting results from a DLS analysis based on intensity fluctuations, but the mean number

TABLE I Latex Mean Diameters by Monomodal Algorithm and Relative Proportion

Analysis	Intensity	Volume	Number
Mean (nm)	307.8	350	316.1
Width	109	146	175
%	100	100	100

diameter also has to be considered, because it can be more easily compared to microscopic results.

Monomodal-Cumulants Model

Here the chosen model is the monomodal one. In Figure 7*a*, the plot of the autocorrelation function G_1 versus sample time, τ, is represented. Function G_1 quantifies the similarity between two acquisitions on a same small suspension volume taken at two different moments separated by τ, the sample time.

When two acquisitions are identical, $G_1(\tau) = 1$, the most information about the suspension is obtained. In the opposite case, when $G_1(\tau)$ equals zero, i.e., when two acquisitions are totally different, no information about the system can be extracted.

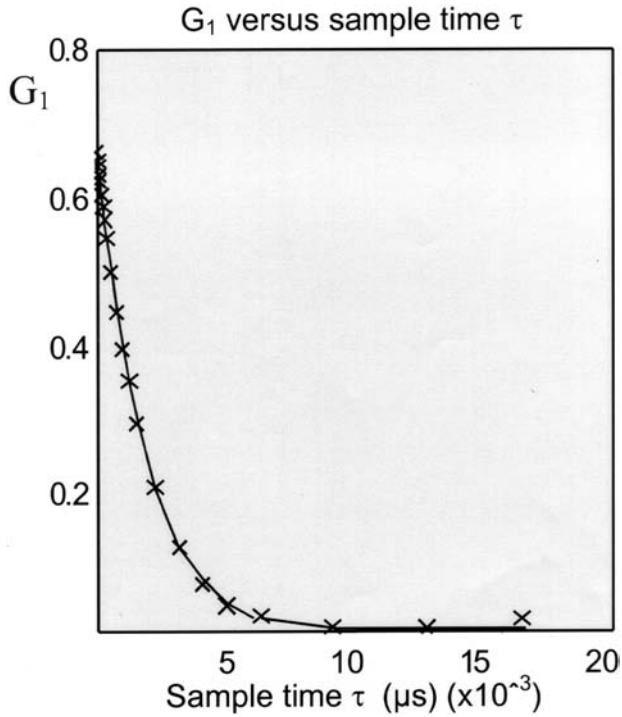

FIGURE 7*a* QELS G_1 autocorrelation function of latexes in a function of the sample time τ fitted by monomodal algorithm (at least five acquisitions of ten subruns, suspension/solvent intensity ratio > 50).

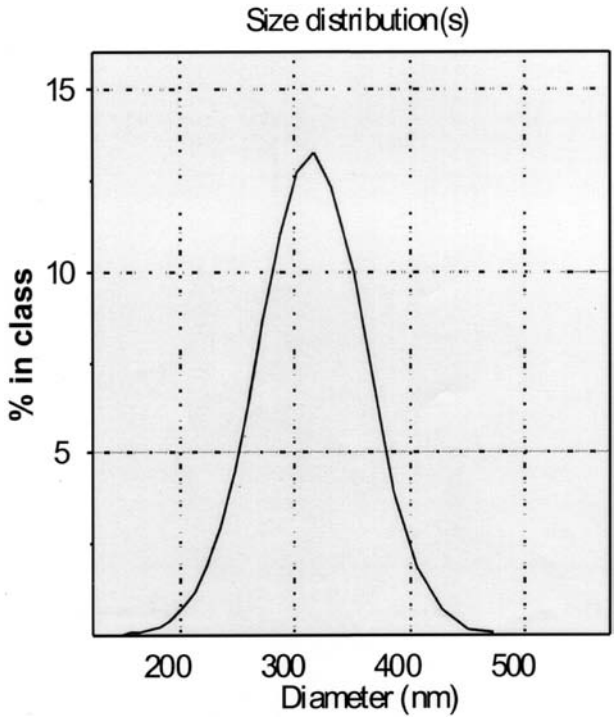

FIGURE 7*b* QELS intensity-average size distribution of latexes obtained by monomodal algorithm (at least five acquisitions of ten sub-runs, suspension/solvent intensity ratio>50).

The first τ for which $G_1(\tau)$ equals zero, is called the relaxaton time, t_r. In other words, the shorter the sample time τ is, the bigger the ratio t_r/τ is, and the better the statistics (number of accumulations) are.

In Figure 7*a*, the experimental data are represented by crosses and fitted by the monomodal model curve. The fit is good for most of the data, and only the data corresponding to the smallest G_1 values are not correctly fitted. The relaxation time, t_r, equals 20 ms, which can be considered as a covenient value.

In Figure 7*b*, the size class distribution in intensity is shown versus the particle diameters analyzed. Only one peak appears centered about 310 nm. It is a Gaussian curve.

Table I shows that the mean intensity value is very close to the one measured by TEM, given by Interfacial Dynamics Corp. However, the measured polydispersity is around 15%. Polydispersity is often an

important parameter for nanoparticles. The mean volume and mean number averages are obtained by calculaton. One can note that the mean number value is very close to the mean intensity one.

Contin Model

The same data may be analyzed via use of the Contin algorithm. G_1 versus sample time and size distribution versus intensity diameters are represented, respectively, in Figures 8*a* and 8*b*. Here, the relaxation time, t_r, is about 30 ms, which is longer than with monomodal cumulant model. As explained below, the shorter the sample time is, the better the statistics are. Thus, the Contin model does not seem to be the most convenient model.

The distribution peak form is not as close as the monomodal treatment to a Gaussian distribution. It proves that the Contin analysis, in this case of a nearly monodisperse sample, is not the more convenient algorithm. The intensity mean diameter, shown in Table II, is not as close to the given standard value 310 nm as the monomodal value. The other mean values are out of range, especially because of their width, which is as large as the diameter itself.

In conclusion, in the DLS study of nearly monodisperse samples, the use of the monomodal algorithm is recommended.

Laser Granulometry Study

The use of laser granulometry requires some caution during sample preparation as mentioned earlier. Similarly to DLS, laser granulometry results are represented as the size distribution versus volume-average diameters. Each sample is diluted with the help of the continuum medium in order to achieve the ideal experimental condition with an adequate obscuration coefficient (about 0.3). Then acquisitions are made until five consecutive runs give similar results, in order to achieve good repeatability.

In Figure 9, the size distribution was observed with the 45 μm focal lens and, in Figure 10, the same observation was carried out with the 100 μm focal lens. With the former, only one population appears centered on 300 nm and, for the latter, four different size classes are observed, with three of them being obviously artifacts. The optical system, in relation to the size range observed, is of great importance if meaningful results are to be obtained.

Table III gives the results of the 45 μm focal measurements. Among the various averaged diameters compiled, which are obtained by different calculations, the two most important are the volume and number representations. The number diameter will be taken into account in the following, since it can be easily compared to microscopy results.

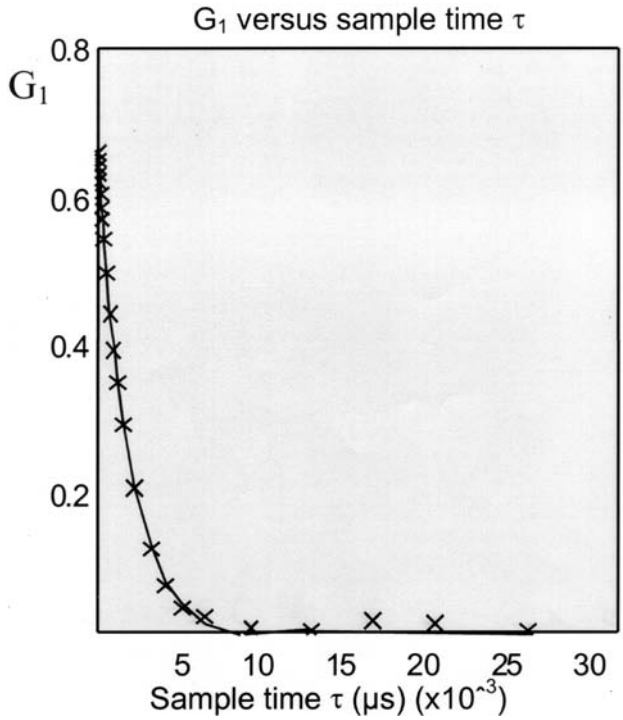

FIGURE 8*a* QELS G_1 autocorrelation function of latexes in a function of the sample time τ fitted by Contin algorithm (at least five acquisitions of ten sub-runs, suspension/solvent intensity ratio >50).

STUDY OF PLANT PROTEIN NANOPARTICLES

The suspension used was a plant protein nanoparticle system described earlier[1]. It was obtained by a coacervation method. The desolvatation of macromolecules was caused by addition of a solvent phase, an ethanolic aqueous solution of the protein, to a nonsolvent phase. The chosen protein is gliadins, extracted from wheat flour. Several techniques were applied, DLS (cumulants and Contin), laser granulometry, and SEM, in order to determinate the most representative distribution for the sample.

DLS Study

The same preparation caution is taken for the DLS sample as described earlier (no pollutants and no multiple scattering). For each sample, at least five acquisitions of ten sub-runs are made. The software

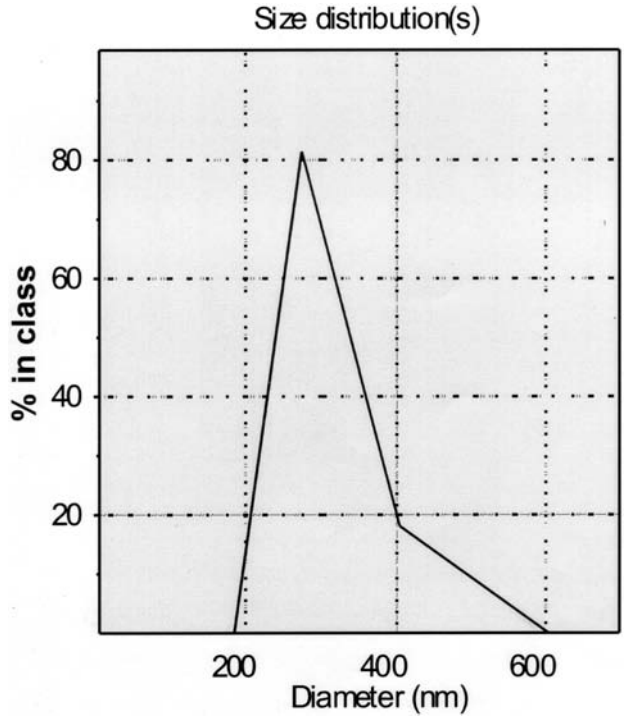

FIGURE 8*b* QELS intensity-average size distribution of latexes obtained by Contin algorithm (at least five acquisitions of ten sub-runs, suspension/solvent intensity ratio > 50).

for each subacquisition checks off the measurement quality for each mathematical treatment (monomodal-cumulants, Contin described later). The intensity ratio suspension/solvent is fifty.

Monomodal-Cumulants Model

The relaxation time, t_r, of the G_1 fit, Figure 11*a*, is large (longer than 100 ms). The application of monomodal model here seems to be poor.

TABLE II Latex Mean Diameters by Contin Algorithm

Analysis	Intensity	Volume	Number
Mean (nm)	297	391	354
Width	131.4	341.9	351.2

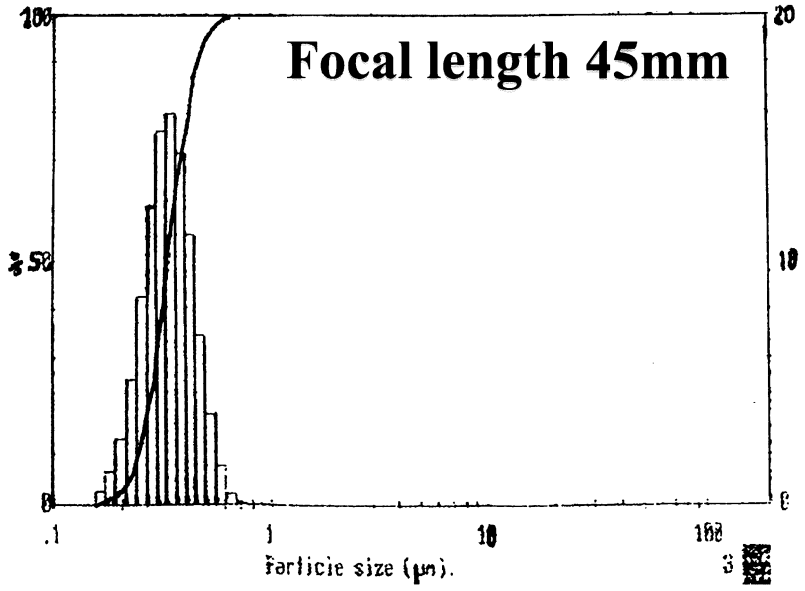

FIGURE 9 Volume-average size distribution of latexes obtained by laser granulometry with the 45 mm focal length (obscuration coefficient around 0.3, five consecutive acquisitions given similar results).

The intensity size distribution, Figure 11*b*, presents one peak, but the number distribution, Figure 11*c*, presents several. Table IV does not give narrow values of the mean diameter. This heterogeneity of results shows that the monomodel assumption is not appropriate for this particular case.

Contin Model

With the Contin analysis, Figure 12*a*, t_r of G_1 is less than 25 ms. The results are better than those from the monomodal-cumulant model. A single peak is seen in the size distribution curve, Figure 12*b*. Its form is nearly Gaussian and it is centered around 800 nm. The mean intensity value is around 800 nm, but the width is important. The two other analyses, in volume and in number, given in Table V, are out of sense and are probably due to calculation artifacts. In fact DLS analysis points out a quite polydisperse population with a mean size greater than λ (i.e., about 800 nm).

To conclude, DLS analysis shows several distributions, with one of them composed of particles larger than λ.

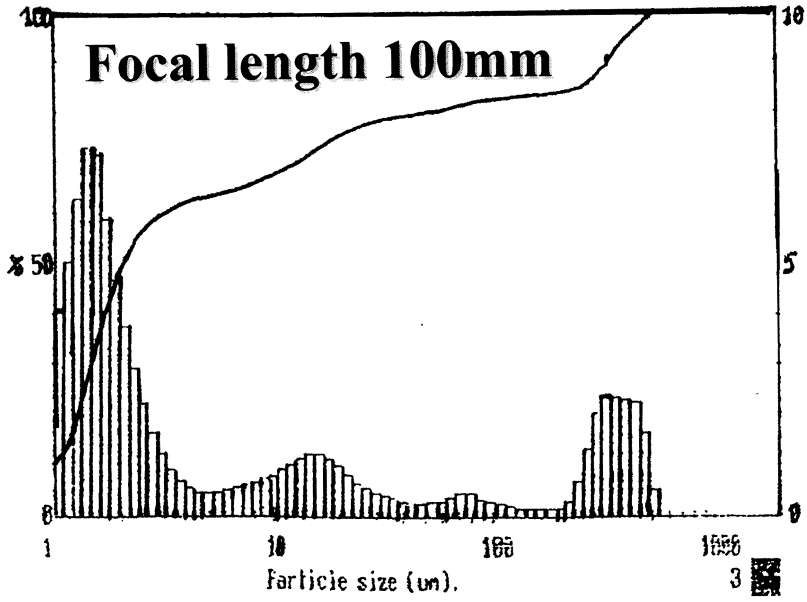

FIGURE 10 Volume-average size distribution of latexes by laser granulometry with the 100 mm focal length (obscuration coefficient around 0.3, five consecutive acquisitions given similar results).

Laser Granulometry Study

From the plant protein nanoparticles suspension, a laser granulometry sample without any pollutants or gas bubbles was prepared. The size distribution plot, Figure 13, shows two size classes: one around 500 nm and another at 6 μm. It is now clear why light scattering was not usable. The latter class represents less than 10% of the sample population. The mean volume diameter is 1 μm while 50% of the particle size are less than 550 nm. These results are coherent, but very different. Let us now consider an SEM image of the particles.

TABLE III Latex Mean Diameters by Laser Granulometry

Analysis	Intensity	Volume
Mean (nm)	340	290
Width	28	21

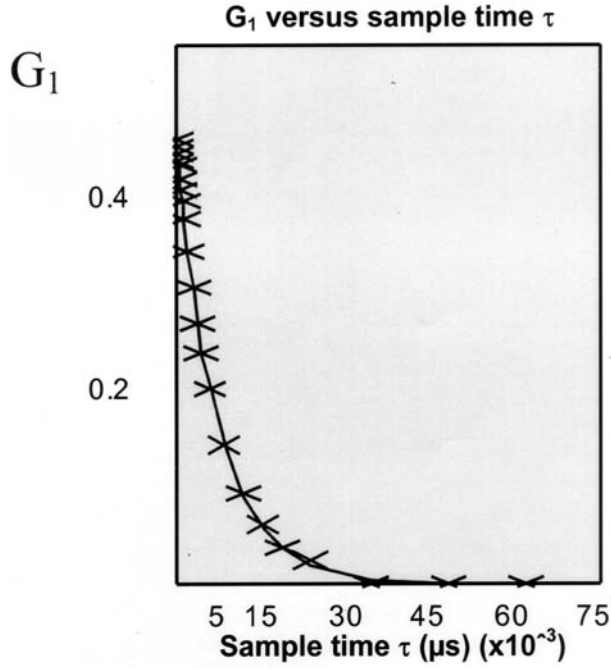

FIGURE 11*a* QELS G_1 autocorrelation function of plant protein nanoparticles fitted by monomodal algorithm (at least five acquisitions of ten sub-runs, suspension/solvent intensity ratio > 50).

SEM

The sample preparation was evaporated in a vacuum chamber, and then the deposition of a colloidal metal was performed. This layer conducts on the sample surface the electron beam and generates the secondary electrons forming the SEM image. Should the beam fuse the particles of gel or of soft polymers, cryo-SEM could be used.

Several micrographs (at least 10) of the same sample are taken. Figure 14 is representative of all of them and shows spherical particles. The diameter of most of them is less than 700 nm in a "dry" state. A few of them are bigger than 2 μm such as the one next to the 1 μm bar. This image confirms the previous results: the Contin DLS diameter of 800 nm, which has been found in the aqueous medium, and the laser granulometry two size classes whose diameters are upper than 1 μm. It would be interesting now to perform an image analysis in order to confirm the four peaks seen by Contin analysis.

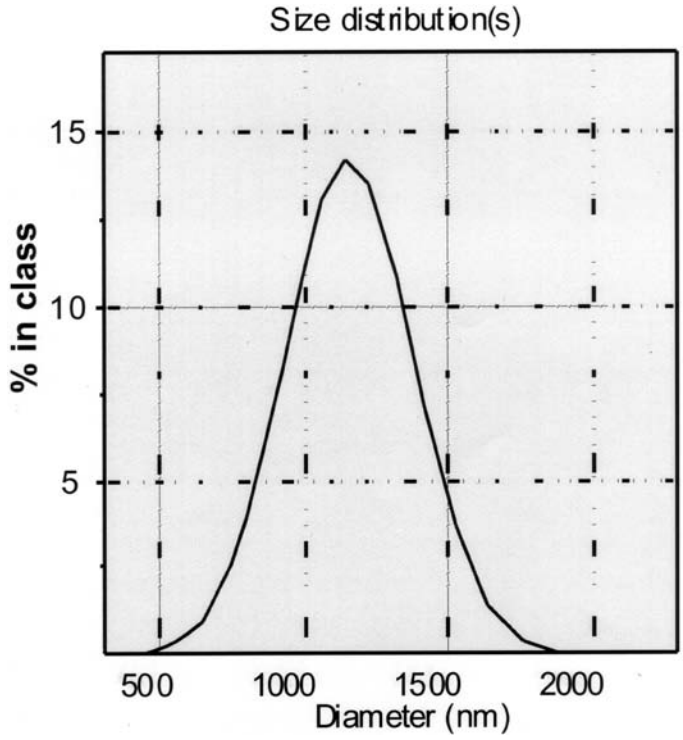

FIGURE 11*b* QELS intensity-average size distribution of plant protein nanoparticles obtained by monomodal algorithm (at least five acquisitions of ten subruns, suspension/solvent intensity ratio > 50).

This example shows that a characterization of nanoparticles size, for such a non-ideal sample, is not evident. The sample polydispersity leads to many difficulties. To resolve them, a solution could be to separate the different size classes, and then to characterize them. Different solutions may also be used, as reviewed in the following section.

POTENTIAL SOLUTIONS TO PROBLEMS ASSOCIATED WITH POLYDISPERSITY

Sedimentation

Generally speaking, sedimentation gives access to information over a wide size range, from a few nanometers up to several micrometers. This is

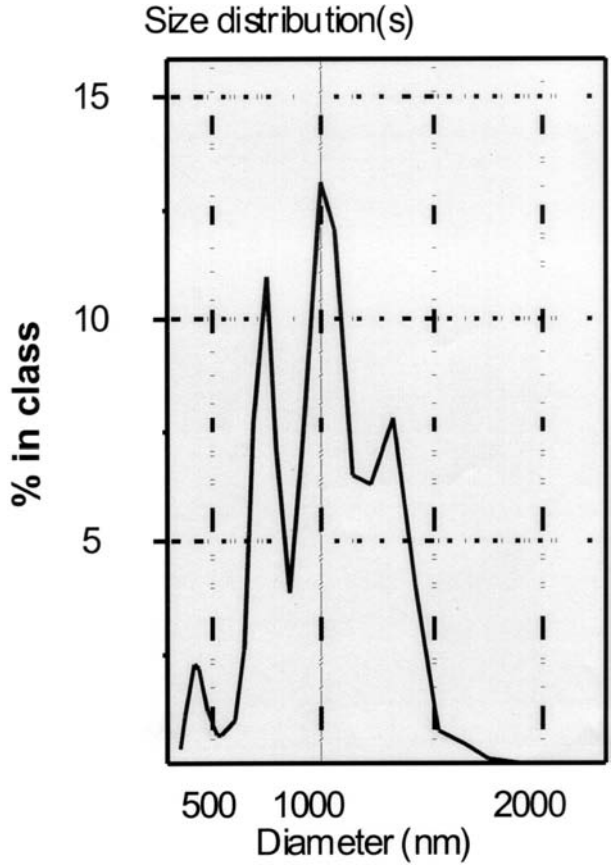

FIGURE 11*c* QELS number-average size distribution of plant protein nanoparticles obtained by monomodal algorithm (at least five acquisitions of ten subruns, suspension/solvent intensity ratio > 50).

especially true with the ultracentrifugation for nanosized objects. With an appropriated optical system, the size analysis is made easier with the help of time used as a separator. A unique size class passes in front of the optical system at any point in time. In fact, monodisperse and uncharged hard spherical particles are quickly size characterized in very diluted suspension if the sedimentation occurs rapidly enough.

These techniques are based on the free and unhindered sedimentation of particles. The potential complicating factors for such a characterization are polydispersity—i.e., size distribution mixture, attractive and charged particles, non-ideal shapes, temperature, dilution shock, vessel

TABLE IV Plant Protein Nanoparticle Mean Diameters by Monomodal Algorithm and Relative Proportion

Analysis	Intensity	Volume			Number			
Mean (nm)	1107.3	752.5	1023.7	1313.2	446.5	738.5	1035.6	1327.7
Width	523.9	120.5	134.5	205	96.8	156	234.5	102.4
%	100	12.4	39.2	47.8	7.3	30.6	44.4	17.7

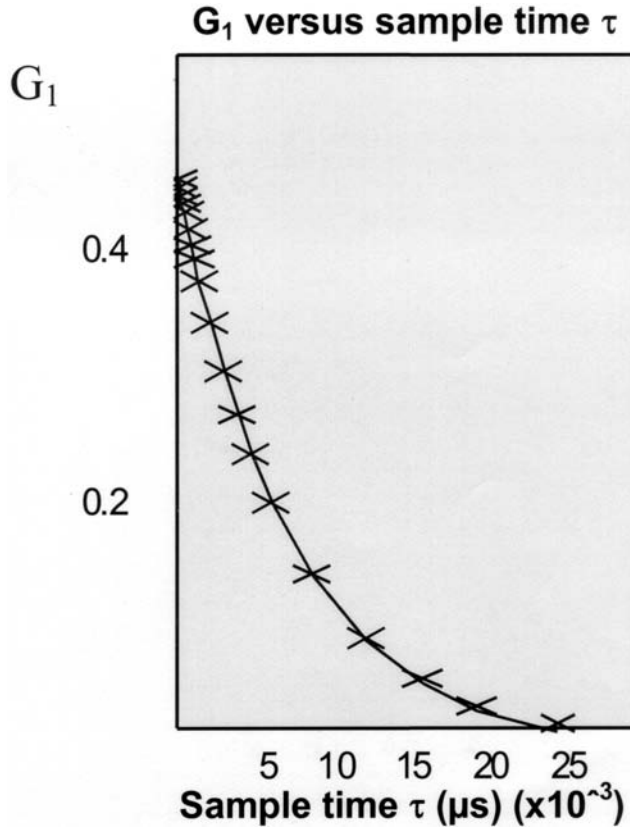

FIGURE 12*a* QELS G_1 autocorrelation function of plant protein nanoparticles fitted by Contin algorithm (at least five acquisitions of ten sub-runs, suspension/solvent intensity ratio > 50).

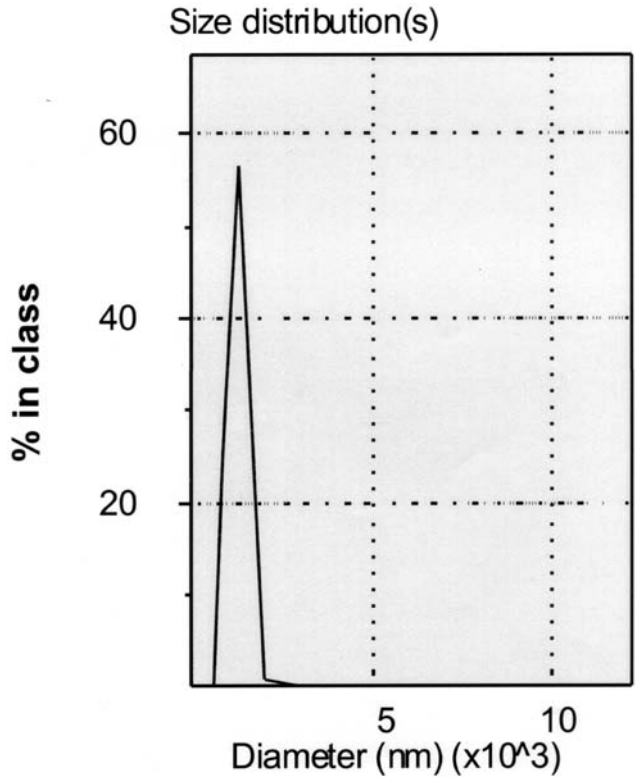

FIGURE 12*b* QELS intensity-average size distribution of plant protein nanoparticles obtained by Contin algorithm (at least five acquisitions of ten sub-runs, suspension/solvent intensity ratio > 50).

geometry, and softness of the particles surface. Nowadays some of these difficulties are partially covered up. Philipse[18] has written an interesting review about this point.

TABLE V Plant Protein Nanoparticles Mean Diameters by Contin Algorithm and their Relative Proportion

Analysis	Intensity		Volume	Number
Mean (nm)	7.8	745.8	1.9	1.3
Width	16.2	1219	0.7	0
%	16.9	83.1	100	100

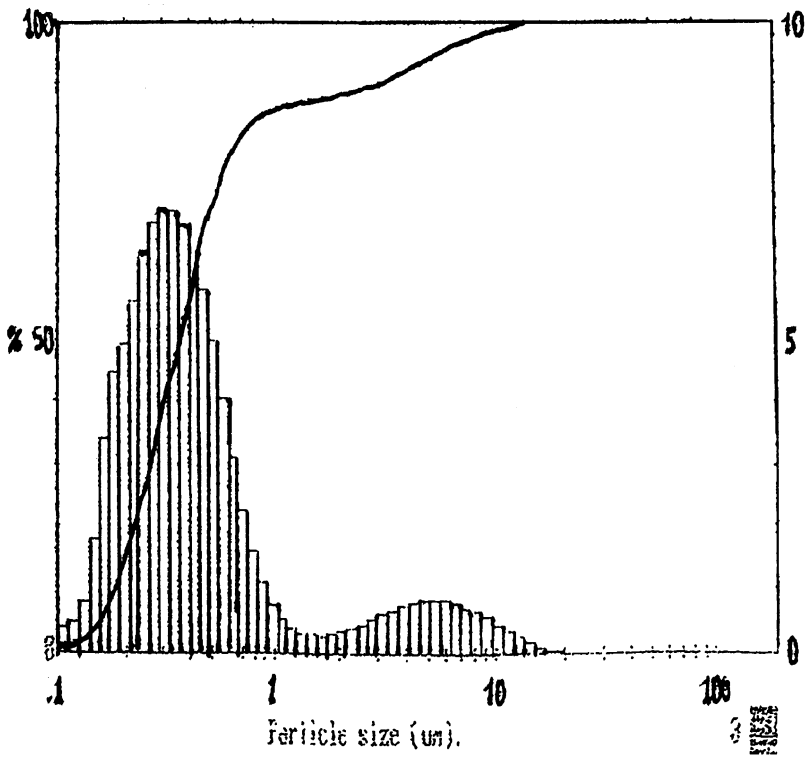

FIGURE 13 Volume-average size distribution of plant protein nanoparticles obtained by laser granulometry with the 45 mm focal length (obscuration coefficient around 0.3, five consecutive acquisitions given similar results).

Another approach, for a very diluted complex sample, is to couple DLS with SLS. This method is known as multiangle dynamic light scattering.

Multiangle Dynamic Light Scattering[19,20]

At different angles, the fluctuation intensities data are cumulated and, then, integrated in two ways: averaged over a period of time (SLS) and time dependent (DLS). The two results are correlated: the dynamical data are evaluated by the Mie scattering function and then related to the statistical intensity values. The obtained results are more reliable than the ones generated only by DLS or SLS. Several classes are now resolved and characterized even if they are close together.

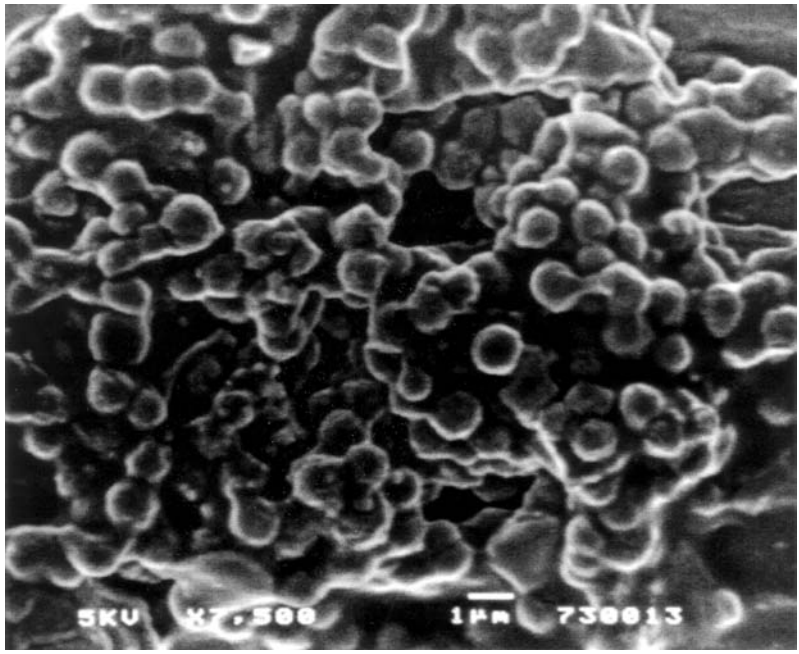

FIGURE 14 Plant protein nanoparticles SEM image.

Another point of view is, first, to separate the size distribution fractions and, then, to analyse them. The separation could occur by one of the flow field fractionation (FFF) family techniques.

Flow Field Fractionation Techniques

FFF methods[21] are direct and non-invasive methods. The different fractions of the polydisperse sample are first separated, and then their mean diameters are evaluated. The separation occurs by differential retention related to a physicochemical parameter difference in a stream liquid flowing through a thin channel (50–300 μm). The separated components are eluted one by one into a detector, often a MALS detector (multi-angle light scattering). The size range spreads from a few nm to 100 μm with the help of the Rayleigh–Debye–Gans and Lorentz–Mie combination algorithms.

Sedimentation Flow Field Fractionation

The discriminating parameter involved in the sedimentation FFF is the specific gravity difference between the particles and the aqueous

phase. A circular channel spins around a centrifuge axis and the species are separated by the radially induced acceleration. For each peak, the retention time is related to the particle size through MALS measurements, and these results could be complemented by other microscopic characterizations.

Sedimentation FFF is not convenient for smaller sized particles (< 30 nm), whose sedimentation process is too slow. In such case, FFF is convenient. The separation in this latter technique is driven by a "cross-flow" field obtained by a second stream at a right angle to the main one.

Environmental Microscopy

Environmental microscopy, as shown earlier, avoids the inconvenience and possible artifacts of "dried" sample. The sample hydration is controlled by varying the vapor pressure in the chamber while maintaining the temperature constant[13]. The thermal conductivity of the sample can be critical. In addition the water can condense or evaporate. Before the pump-down sequence, the chamber has to be saturated to minimize the sample water evaporation. This microscopy method needs no prior sample preparation[18]. The image is a picture of nanoparticles; this method is less invasive than SEM and the diameters are reliable. With the use of an image analysis, the size distribution curve is easily obtained. Such a method affords direct particle observation in their own medium without any dilution.

CONCLUSION

The different examples presented show that size characterization is not such an easy analysis especially with a complex sample composed of several size populations.

Nanosized objects are observable by many techniques. Most of them are adversely affected by concentrated conditions, polydisperse distributions, and irregular particle shapes. Multiangle dynamic light scattering can be very helpful in overcoming the last two disadvantages.

The concentration dependency is avoided by eluting and by separating each size class before identifying them. For instance, multiangle dynamic light scattering is fruitfully coupled with sedimentation FFF. In this case, the particles are observed by indirect ways, for example light intensity fluctuations.

Particles are directly seen by methods such as electronic microscopy. The major disadvantage of these techniques is that the particles are not characterized in solution but in a "dried" state, environmental microscopy being an exception. This method is a less invasive technique and gives results that are most representative of the real sample size

distribution if it is coupled with an image analysis. Its development seems to be very promising in the next decades, but currently it is rarely applied.

Finally, to prevent making excessive assumptions, the preferred solution is to couple several size characterization techniques. It is preferred that at least one *in situ* technique be combined with electronic microscopy.

REFERENCES

[1] Duclairoir, C., Irache, J. M., Nakache, E., Orecchioni, A.-M., Chabenat, C., and Popineau, Y. (1999), *Polymer International*, **79**, 327.

[2] Pusey, P. N. (l973). In: *Industrial Polymers: Characterization by Molecular Weight*, J. H. S. Green and R. Dietz, Ed. (Transcripta Books: London).

[3] Atkins, P. W. (1999). In: *Physical Chemistry, 4th ed.* (Oxford University Press: Oxford, UK).

[4] Rayleigh, L. (187l). *Phil. Mag.*, **41**, 107, 274, 447.

[5] Kralchevsky, P. A., Danov, K. D., Denkov, N. D. (l997). In: *Handbook of Surface and Colloid Chemistry*. K. S. Birdy, Ed., 448–494 (CRC Press: Boca Raton, Florida).

[6] Debye, P. (1915). *Ann. Phys.*, **46**, 809.

[7] Gans, R. (1921). *Ann. Phys.,* **65**, 37; (1923). *Ann. Phys.,* **67**, 353; (1925). *Ann. Phys.,* **76**, 29.

[8] Mie, G. (1908). *Ann. Phys.*, **25**, 377.

[9] Carr, W. (1976) In: *Progress in Organic Coatings*, **4**, 161.

[10] McClements, D. J., and Coupland, J. N. (1996). *Colloids and Surfaces A*, **117**, 161.

[11] Chestnut, M. H. (1997). *Current Opinion in Colloid & Interface Science*, **2**, 158.

[12] Donald, A. M. (1998). *Current Opinion in Colloid & Interfaces Science*, **3**, 143.

[13] Griffith, E., and Newbury, D. E. (1996). *Scanning*, **18**, 465.

[14] Wyatt, P. J. (1998). *Journal of Colloid & Interface Science*, **197**, 9.

[15] Fennell, E. D., and Wennerström, H. (1994). In: *The Colloidal Domain Where Physics, Chemistry, Biology, and Technology Meet* (VCH Editions: New York).

[16] Stepanek, P. (1993). In: *Dynamic Light Scattering*, W. Brown, Ed., pp. 177–241 (Oxford University Press: Oxford, UK).

[17] Provencher, S. W. (1982). *Comput. Phys. Comm.,* **27**, 213–227.

[18] Philipse, A. (1997). *Current Opinion in Colloid & Interface Science*, **2**, 200.

[19] Bryant, G., and Thomas, J. C. (1995). *Langmuir*, **11**, 2480.

[20] Bryant, G., Abeynayake, C., and Thomas, J. C. (1996). *Langmuir*, **12**, 6224.

[21] Giddings, J. C. (1993). *Science*, **260**, 1456.